Published in final edited form as:
Gastroenterology. 2011 February ; 140(2): 560–571. doi:10.1053/j.gastro.2010.10.042.

D-Glucose Acts via SGLTI to Increase NHE3 in Mouse Jejunal Brush Border by a NHERF2-Dependent Process

Rong Lin[a,b,+], **Rakhilya Murtazina**[a], **Boyoung Cha**[a], **Molee Chakraborty**[a], **Rafiquel Sarker**[a], **Tian-e Chen**[a], **Zhihong Lin**[a], **Boris M. Hogema**[c], **Hugo R. de Jonge**[c], **Ursula Seidler**[d], **Jerrold R. Turner**[e], **Xuhang Li**[a], **Olga Kovbasnjuk**[a], and **Mark Donowitz**[a,f]

[a] Department of Medicine, Division of Gastroenterology, Johns Hopkins University School of Medicine, Baltimore, Maryland, USA [b] GI Division, Wuhan Union Hospital, Tongi Medical School, Huazhong University of Science and Technology, 1277 Jiefang Road, Wuhan, China [c] Department of Biochemistry, Erasmus University Medical Center, Rotterdam, Netherlands [d] Department of Gastroenterology, Hannover Medical School, Hannover, Germany [e] Department of Pathology, The University of Chicago, Chicago, Illinois, USA [f] Department of Physiology, Division of Gastroenterology, Johns Hopkins University School of Medicine, Baltimore, Maryland, USA

Abstract

Background & Aims—Oral rehydration solutions (ORS) reduce diarrhea-associated mortality by unclear mechanisms. Sodium absorption is mediated by the Na^+/H^+ hydrogen exchanger NHE3 and is increased by Na^+-glucose co-transport in vitro, but the mechanisms of this process are only partially understood and its in vivo relevance has not been determined.

Methods—Intracellular pH was measured in jejunal enterocytes of wild-type mice and mice with disrupted *Na+/H+ exchange regulatory co-factor 2* (*NHERF2*−/− mice) by multi-photon microscopy. Diarrhea was induced by cholera toxin. Caco-2BBe cells that express NHE3 and the sodium/glucose cotransporter (SGLT)1 were studied by fluorometery, before and after siRNA-mediated knockdown of NHERF1 or NHERF2. NHE3 distribution was assessed by cell-surface biotinylation and confocal microscopy. Brush border mobility was determined by fluorescence recovery after photobleaching and confocal microscopy.

Results—The non-metabolized SGLT1 substrate α-methyl-D-Glu (α-MD-G) activated jejunal NHE3; this process required Akt and NHERF2. α-MD-G normalized NHE3 activity after cholera toxin-induced diarrhea. α-MD-G–stimulated jejunal NHE3 activity was: defective in *NHERF2*−/− mice and cells with *NHERF2* knockdown, but occurred normally with *NHERF1* knockdown; associated with increased NHE3 surface expression in Caco-2 cells, which was also NHERF2-dependent; associated with dissociation of NHE3 from NHERF2 and an increase in the NHE3

Address for correspondence: Mark Donowitz and Rong Lin, Johns Hopkins University School of Medicine, 720 Rutland Avenue, 925 Ross Research Building, Baltimore, MD 21205. Phone: 410-955-9675; fax: 410-955-9677. mdonowit@jhmi.edu.
[+]Current address: GI Division, Wuhan Union Hospital, Tongi Medical School, 1277 Jiefang Road, Wuhan, China

Author Contributions: RL designed and performed all studies. Others assisted in: RM, ZL, OK multiphoton microscopy. BC FRAP studies. RS, TC and MC gradient centrifugation studies. BH, HJ, US, JT and MD supervision and discussions of the strategies and writing of manuscript.

No author has a conflict of interest.

mobile fraction from the brush border; and accompanied by a NHERF2 ezrin-radixin-moesin–binding domain-dependent increase in co-precipitation of ezrin with NHE3.

Conclusions—SGLT1-mediated Na-glucose co-transport stimulates NHE3 activity in vivo by an Akt- and NHERF2-dependent signaling pathway. It is associated with increased brush border NHE3 and association between ezrin and NHE3. Activation of NHE3 corrects cholera toxin-induced defects in Na absorption and might mediate efficacy of ORS.

Keywords

Intestinal Na absorption; cholera toxin; trafficking; Exocytosis; Ezrin; NHERF2

INTRODUCTION

The human small intestine absorbs approximately 7.5 liters of water and 650 mEq of Na daily. Most of this is accomplished by cotransport of Na and nutrients, particularly D-glucose, and neutral NaCl absorption which is the BB Na/H exchanger 3 (SLC9A3) linked to a Cl/HCO_3 exchanger, either SLC26A3 or A6 [1]. These two processes were assumed to be separate until recent in vitro studies using polarized intestinal epithelial cell monolayers demonstrated enhanced NHE3 activity and surface expression following SGLT1-mediated Na-glucose cotransport [2–5]. However, whether SGLT1-dependent NHE3 activation occurs in vivo under basal or pathologic conditions has not been explored. If present in vivo, this NHE3 activation may represent a mechanism by which ORS stimulates intestinal Na and water absorption.

In vitro studies suggested that SGLT1-dependent NHE3 activation occurs via sequential activation of p38 MAP kinase/MAPKAPK2, Akt2 and ezrin. NHE3 regulation involves signaling complexes that form on the NHE3 C-terminus, many of which are scaffolded by NHERF proteins, a multi-PDZ domain containing gene family [9]. It is unknown whether NHERF proteins are necessary for the SGLT1-NHE3 linkage. The studies presented here used mouse jejunum with NHERF2 KO and Caco-2/SGLT1/HA-NHE3 cells with NHERF2 KD to explore whether α-MD-G stimulates NHE3 in intact tissue and whether the effect requires NHERF2, as well as the mechanism involved in these effects. These results suggest that optimization of the physiologic NHE3 regulatory pathway identified may increase the utility of ORS solutions for severe diarrheal diseases.

Materials and Methods

Animals

Male NHERF2−/− mice bred into the C57BL/6 background (Charles River Laboratories, Inc. Wilmington, MA) for at least six generations were produced from heterozygotes and with wild type male C57BL/6 mice were studied between 10–12 weeks of age. These mice were initially produced by a retroviral trapping method by Lexicon Pharmaceuticals using Omnibank clone OST2298[10]. Protocols used were approved by the JHU Animal Use Committee.

NHE3 Activity Determination by Two-Photon Microscopy

Na+/H+ Exchange Activity in intact mouse jejunum was determined as rates of Na+-dependent alkalinization using a two-photon microscope (MRC-1024MP, Bio-Rad, Hercules, CA) and the pH sensitive dye, SNARF-4F as we have described [11] with minor modifications. Details are provided in Supplementary Methods. Full thickness jejunum was studied starting I cm distal to the ligament of Treitz.

Cholera Toxin-Induced Acute Watery Diarrhea Model

An acute watery diarrhea model using purified holo-cholera toxin (CT, Sigma, St. Louis, MO) was standardized in vivo, as previously described [12]. Mice were gavaged with cholera toxin (10 μg in 7% NaHCO3) through an oro-gastric feeding tube, with NaHCO3 as control. 6 hours later, mice were sacrificed and fluid was collected by gravity from the entire small intestine.

Measurement of NHE3 Activity in Caco-2/bbe Cells

Caco-2 cells stably transfected with SGLT1[3] were infected with HA-NHE3 adenovirus (see Supplementary Methods), grown on pieces of polycarbonate membranes (0.4-μm pore size, called "flilterslips") and NHE3 activity determined using the intracellular pH-sensitive dye BCECF-AM (2′,7′-Bis(2-carboxyethyl) -5(6)-carboxy fluorescein acetoxymethyl ester, InVitrogen, Carlsbad, CA) and a computerized fluorometer, as described [13]. Na+/H+ exchange rates (H+ efflux) were calculated as the initial rates of Na+-dependent change in pHi over ~1 min (ΔpH/Δmin) [13]. Means ± SE were determined from at least three independent experiments.

Apical Cell Surface Biotinylation of NHE3 in Caco-2/bbe Cells

The Caco-2/bbe cell surface biotinylation protocol was modified from the protocol for PS120 cell surface biotinylation published previously using NHS-SS biotin (Pierce Chemicals) [14]. The details are proved in Supplementary Methods. The immunoblots produced were probed with a monoclonal anti-HA antibody (Covance 16B12, Princeton, NJ), with normalization to β-actin using monoclonal anti-β-actin antibody (Sigma A2228)

Immunoprecipitation and co-precipitation and **Immunofluorescence** techniques are described in Supplementary Methods.

Fluorescence recovery after photobleaching/confocal microscopy was performed as described [10] and is detailed in Supplementary Methods.

Statistics

Results were expressed as mean ± S.E.M. Statistical evaluation was performed by analysis of variance (ANOVA) or Student's t test.

Results

α-MD-G stimulates NHE3 activity in mouse jejunum via SGLT-1

NHE3 activity in intact mouse jejunum was measured by two-photon microscopy using the pH sensitive dual emission dye, SNARF-4F [11,15]. Because the fluorescence of SNARF-4F in different solutions and intracellular conditions often differs, the PKa of SNARF-4F in jejunum was measured by the K+/nigericin(10 mM) method [11]. Supplementary Fig. 1 shows the jejunal calibration of the pH response. Jejunum was sequentially perfused with TMA (20 min) and then Na buffer containing either D-mannose or α-MD-G (25 mM) (Fig 1A). α-MD-G is a non-metabolized analogue of D-glucose and is specifically transported by SGLT1. Fig. 1B shows the pH-dependent emission shifts from acidic to basic, comparing conditions before and after Na+ treatment. Compared with the D-mannose group, α-MD-G significantly stimulates NHE3 activity (0.45 ± 0.03 ΔpH/min *(n=9)* vs. 0.31±0.03 ΔpH/min *(n=5)*, $p<0.01$) (Fig. 1C). The specific SGLT1 inhibitor phloridzin (1 mM) abolished the α-MD-G induced stimulation (0.45±0.03 ΔpH/min *(n=9)*, α-MD-G/no phloridzin vs. 0.21±0.02 *(n=3)*, α-MD-G/phloridzin, $p<0.01$). These results

demonstrate that luminal α-MD-G stimulates NHE3 activity in intact mouse jejunum by a mechanism involving SGLT1.

Akt is an intermediate in D-Glucose stimulation of jejunal NHE3 activity

We next tested the hypothesis that Akt signaling was involved in α-MD-G/SGLT1 dependent NHE3 stimulation in vivo. The Akt inhibitor viii (10 μM) was used, which selectively inhibits Akt 1 and 2 without effects on other closely related AGC kinases [16]. Preincubation with the Akt inhibitor (90 min exposure) caused a slight but non-significant decrease in basal NHE3 activity in the presence of mannose (0.31 ± 0.03 ΔpH/min without *(n=4)* vs. 0.26 ± 0.03 ΔpH/min with Akt inhibitor *(n=3), N.S.) (*Fig. 1C). In contrast, the Akt inhibitor prevented the α-MD-G stimulation of NHE3 activity (0.45±0.03 ΔpH/min *(n=9) without* vs. 0.27 ± 0.03 ΔpH/min *(n=4) with* Akt inhibitor, $p<0.05$). Note, that α-MD-G stimulated NHE3 activity in the presence of Akt inhibitor viii, was not significantly higher than in the presence of phloridzin.

α-MD-G reverses the inhibition of NHE3 activity in an acute cholera toxin-diarrhea model

Whether cholera toxin (CT)-induced inhibition of NHE3 activity could be reversed by α-MD-G was determined. Small intestinal water output was increased 6 h after CT gavage (Fig 2A) (control, 0.86 ± 0.25 ml/mouse (n=3) vs. CT, 2.05 ± 0.25 ml/mouse (n=4), $p < 0.05$). With mannose (Fig. 2B), NHE3 activity was significantly decreased in the CT-treated group (control, 0.30 ± 0.04 ΔpH/min *(n=5)* vs. CT, 0.17 ± 0.01 ΔpH/min *(n=3)* $p<0.05$). However, α-MD-G increased NHE3 activity in both groups, and NHE3 activity with CT was returned entirely to the level in the control group (control, 0.44 ± 0.02 ΔpH/min *(n=5)* vs. CT, 0.38 ± 0.05 ΔpH/min *(n=4), N.S.*). Boiled CT did not alter jejunal NHE3 activity when mannose was present. The increment of NHE3 activity caused by α-MD-G was larger in the CT exposed than in the control group (112% increment in CT vs 56% in control group), consistent with there being reversal of the cholera toxin-induced inhibition of NHE3 activity by α-MD-G.

α-MD-G stimulation of NHE3 is associated with shifting of NHE3 into smaller complexes

The mechanism of α-MD-G stimulation of jejunal NHE3 was examined by determining whether this effect was associated with changes in the size of NHE3 containing complexes. Changes in NHE3 activity due to altered signaling are often associated with changes in NHE3 complex size due to changes in NHE3 associating proteins [8]. Total jejunal membranes exposed to mannose vs α-MD-G were solubilized in 1% Triton X-100 and placed on 5–30% discontinuous sucrose density gradients. NHE3 complex size was determined by immunoblotting. α-MD-G stimulation of NHE3 activity was associated with shifting of NHE3 into smaller sized complexes (Supplementary Fig. 2), consistent with changes in NHE3 associating proteins. This is the first model of NHE3 regulation in which NHE3 complex size is decreased.

α-MD-G stimulation of NHE3 activity is NHERF2 dependent in Caco-2/SGLT1 cells and intact mouse jejunum

NHERF1 and 2 have been shown to be necessary for multiple aspects of NHE3 regulation and complex formation. Given the change in NHE3 complex size caused by α-MD-G, we evaluated the role of NHERF1 and 2 in α-MD-G stimulated NHE3 activity. Lentiviral shRNA-puromycin vectors were used to knock down NHERF1 and NHERF2 in Caco-2 cells. Stable cells lines were established in which the expression of the knockdown constructs and the effects of the knockdowns lasted > ten passages. Fig. 3A demonstrates the successful KD of NHERF1 and NHERF2 by 70–80%.

α-MD-G caused similar NHE3 stimulation in Caco-2 cells expressing the control (GFP oligomers) and NHERF1 KD constructs (Figs. 3B left and middle, respectively). However, in NHERF2 KD cells, α-MD-G did not significantly alter NHE3 activity (Fig. 3B, right). Of note, NHE3 activity in NHERF1 KD cells (0.14 ± 0.01 ΔpH/min n=4) was significantly decreased compared to control cells (0.25 ± 0.02 ΔpH/min, n=12 ($p<0.05$)), while NHE3 activity was significantly increased in NHERF2 KD cells (0.33 ± 0.02 ΔpH/min, n=5, ($p<0.05$); all these results from Fig 3B were in the presence of mannose).

The NHERF2 dependence of α-MD-G-induced NHE3 stimulation on NHE3 was also confirmed using NHERF2 knock out mouse jejunum. Shown in Fig. 3C, NHE3 activity was not significantly altered in D-mannose vs. α-MD-G perfused jejunum in these NHERF2 KO mice (0.36 ± 0.03 ΔpH/min *(n=6)* vs. 0.39 ± 0.02 ΔpH/min *(n=5)*). These results show that α-MD-G stimulation of NHE3 is NHERF2-dependent in both intact small intestine and Caco-2 cells.

NHERF2 is necessary for α-MD-G stimulated NHE3 activity by regulating its plasma membrane trafficking

To determine the basis of the α-MD-G stimulation of NHE3 activity, the amount of BB NHE3 was determined using cell surface biotinylation. α-MD-G increased the amount of NHE3 on the cell surface in Caco-2 control cells (intensity of NHE3 on cell surface normalized with β-actin, 0.46 ± 0.03), compared with D-mannose conditions (0.32 ± 0.04, $p<0.05$) (Fig 4). In contrast, in Caco-2-NHERF2 KD cells, with or without the presence of α-MD-G, the surface NHE3/actin was similar (0.50 ± 0.03 vs. 0.48 ± 0.6, NS). This result suggests that NHERF2 is involved in α-MD-G stimulated NHE3 activity by affecting trafficking to increase the amount of BB NHE3.

The surface NHE3/actin under D-mannose conditions was increased in the NHERF2 KD compared to D-mannose conditions in Caco-2 control cells (0.48 ± 0.01 vs. 0.32 ± 0.04, $p<0.05$, Fig. 4A). This is consistent with the increased NHE3 activity seen under these conditions (see Fig. 3B, D-mannose-shRNA$_i$-GFP vs. NHERF2 KD). We will speculate on the explanation below.

To investigate further whether NHERF2-dependent trafficking is involved in α-MD-G dependent stimulation of NHE3, confocal microscopic XZ images were generated. We confirmed that α-MD-G increased the percentage of NHE3 localized to the apical domain of Caco-2 cells as indicated by co-localization with wheat-germ agglutinin (WGA), which stains only the apical membranes of confluent monolayers at 4°C. Under basal conditions (mannose), 57.8 ± 4.0% of NHE3 co-localized with WGA (n=21) in the plasma membrane of Caco-2/HA-NHE3 cells, and this percent overlap increased to 82.4 ± 4.0% 5 min after α-MD-G treatment (n=14) (Figs. 5A and 5B, left). In contrast, the stimulation of NHE3 translocation to the plasma membrane by α-MD-G was abolished when NHERF2 was knocked down in Caco-2 cells (overlap of WGA/NHE3 with mannose exposure 74.7 ± 3.0% (n=17) vs. α-MD-G 74.2 ± 5.2% (n=16), NS) (Figs. 5A and 5B, right).

α-MD-G-induced stimulation of NHE3 is associated with dissociation of NHE3 from NHERF2

In mannose conditions in Caco-2/NHERF2 KD cells, there was more NHE3 co-localized with apical WGA compared to the control cells (Fig. 5B). This result suggests that the α-MD-G regulation of NHE3 trafficking involves dissociation of NHE3 from this pool of NHERF2. This finding was confirmed using double immunofluorecence staining of NHE3 and NHERF2 in Caco-2 cells (Figs. 6A,B). The colocalization of NHE3 and NHERF2 was decreased from 62.8 ± 1.7% (n=4) to 53.4 ± 1.4% (n=4,) ($p<0.05$) by α-MD-G treatment.

Co-immunoprecipitation studies were performed to further demonstrate the dissociation of NHE3 and NHERF2 (Fig. 6C). Caco-2/NHERF2 KD cells were transfected with Flag-NHERF2 full length and Flag-NHERF2 Δ30 separately. In Caco-2 cells expressing Flag-NHERF2, after α-MD-G there was less FLAG-NHERF2 co-immunoprecipitated with NHE3. This further confirmed the α-MD-G-induced NHERF2-NHE3 dissociation. In contrast, in Caco-2 cells expressing Flag-NHERF2Δ30, which lacks the NHERF2 ezrin binding domain, α-MD-G did not decrease NHE3-NHERF2 binding. Moreover, α-MD-G failed to stimulate NHE3 activity in Caco-2 cells expressing NHERFΔ30 (Fig. 6D). This indicates that ezrin binding to NHERF2 is required for α-MD-G-induced NHERF2-NHE3 dissociation, which is needed for α-MD-G to increase NHE3 activity.

Stimulatory effect of α-MD-G on NHE3 mobile fraction is dependent on NHERF2

We have previously reported there are two different pools of apical domain NHE3; a mobile and an immobile pool under basal conditions, with stimulation of NHE3 associated with an increase in the mobile BB pool [17]. FRAP/confocal microscopy was used to determine whether the α-MD-G stimulation of NHE3 was associated with a dynamic effect on the mobile fraction of apical NHE3, and whether NHERF2 was required for this effect. Caco-2 cells transiently expressing NHE3-GFP with endogenesis NHERF2 or with NHERF2 KD were used to perform FRAP. 5 mins after mannose or α-MD-G treatment, images were recorded before and every 30 seconds after bleach for up to 20 mins. Supplementary Fig 3A shows a representative experiment and Supplementary Fig 3B shows means +/−SEM with fluorescent intensity determined before and after photobleaching of NHE3. The mobile fraction of NHE3 under basal conditions in the presence of mannose was ~10% (obtained by curve-fitting), which was dramatically enhanced to ~30% with α-MD-G exposure. Caco-2/NHERF2 KD cells with mannose exposure exhibited an increased NHE3 mobile fraction compared with Caco-2 cells expressing NHERF2 (21.4±3.2 vs. 9.7±1.2 (%)). Importantly, α-MD-G did not increase the NHE3 mobile fraction in these Caco-2/NHERF2 KD cells (21.4±3.2 vs. 20.1±4.1 (%)). These results show that α-MD-G stimulates the NHE3 mobile fraction in the Caco-2 apical domain by a NHERF2 dependent process.

α-MD-G-induced NHE3 stimulation is associated with increased phosphorylation of ezrin at a step prior to NHERF2

As shown above, ezrin binding to NHERF2 is necessary for α-MD-G stimulation of NHE3 (Fig. 6D). The mechanism of ezrin's role was studied. α-MD-G increased ezrin phosphorylation in all of the cell lines in Fig. 7A, including those with NHERF2 KD and with NHERF2Δ30. This also occurred in both WT and NHERF2 null jejunum (Fig 7B). These results indicate α-MD-G initiated ezrin phosphorylation occurs prior to/independently of the NHERF2 role in NHE3 stimulation.

α-MD-G increases co-precipitation of NHE3 and ezrin, which is NHERF2 dependant

The functional significance of the α-MD-G induced increase in p-ezrin was studied in Caco-2 WT and NHERF2 KD cells. IP NHE3 co-precipitated ezrin the amount of which was increased by treatment with α-MD-G in WT but not NHERF2 null jejunum (Fig 7C) and in Caco-2 cells expressing NHERF2 but not when NHERF2 was KD (Fig. 7D).

Direct ezrin-NHERF2 binding is required for α-MD-G-induced stimulation of NHE3-ezrin association

To determine whether NHERF2-ezrin binding was necessary for the NHE3-ezrin association, as it was necessary for α-MD-G stimulation of NHE3 activity (Fig 6D), Caco-2/WT NHERF2 vs. NHERF2 Δ30 cells were compared for the magnitude of the α-MD-G increase in NHE3 co-precipitation of ezrin. NHE3 co-precipitation of ezrin was increased by

α-MD-G when the Caco-2 cells expressed NHERF2 but not when they expressed NHERF2 Δ30 (Fig 7E). These results show that NHERF2 binding to ezrin is necessary for the α-MD-G stimulation of the NHE3-ezrin association as well as for the stimulation of NHE3 activity.

Discussion

This study revealed 1) α-MD-G stimulates NHE3 activity and increases BB NHE3 amount in mouse jejunum via SGLT1 which a pathway that involves Akt, NHERF2, and ezrin. 2) α-MD-G entirely reversed the inhibition of NHE3 in an acute cholera toxin diarrhea model. 3) NHERF2 is involved in α-MD-G-initiated NHE3 stimulation through regulation of NHE3 trafficking and distribution of NHE3 over the microvillus. 4) Separate ezrin pools participate in two steps of α-MD-G-induced NHE3 stimulation.

This study provides insights in how D-glucose stimulates Na and water absorption from ORS and is relevant to the longstanding observations that the stoichiometry of Na+ absorption from ORS seems to exceed that predicted from the amount of substrate absorbed [18]. Previous explanations implicated solvent drag and included a controversial observation that these solutions altered tight junction permeability/permselectivity [18]. Our study confirmed that in intact jejunum, luminal α-MD-G increased NHE3 activity and this effect occurred entirely via SGLT1, since it was phloridzin inhibitable.

Since diarrheal diseases are almost always at least partially due to inhibition of small intestinal brush border NHE3 activity, often but not always along with stimulation of Cl secretion via CFTR, we tested the hypothesis that stimulation of NHE3 induced by D-glucose would reverse the changes in Na absorption in a diarrheal disease model which acts by elevation of adenylate cyclase-cAMP. α-MD-G totally reversed the CT inhibition of NHE3. Stimulation of NHE3 activity in the CT-exposed intestine exceeded the NHE3 stimulation in control intestine which resulted in the NHE3 activity in the presence of α-MD-G being the same in CT-exposed and control small intestine. This is the first report showing that an agonist which is effective in regulating normally functioning NHE3, is also able to stimulate cAMP-inhibited NHE3 activity. This not only provides insights into the mechanism by which ORS increases water absorption in diarrhea but also has implications for strategies for development of improved treatment of acute diarrheal diseases.

The NHERF family has been reported to be present in and/or close to the BB and to scaffold a variable series of proteins in forming NHE3 complexes in a dynamic manner, which often affect NHE3 activity[7,19]. siRNA knockdown was used to explore which NHERF subtype was involved, revealing a role for NHERF2 but not NHERF1 in α-MD-G stimulation of NHE3 in Caco-2 cells, a dependence that was confirmed by studies in the NHERF2 null mouse jejunum. NHERF2 is present in the apical domain of intestinal Na+ absorptive cells and renal proximal tubules in the mid to lower microvillus, intervillus cleft area and sub-apically, as well as having a cytosolic component [19]. We identified two roles for NHERF2 in α-MD-stimulation of NHE3. It is necessary for 1) the increase in BB NHE3 amount and activity and 2) the increase in the BB mobile fraction of NHE3, which we have suggested is involved in distributing NHE3 over the microvilli [17,20]. The latter correlates with dissociation of NHE3-NHERF2. Under basal conditions, NHERF2 maintains NHE3 in an inactive pool (Fig 3C compared to Fig 3A) that is not in the BB (not being accessible to apically added WGA and biotin (Figs 4 and 5)). We suggest that this pool of NHE3 is in the subapical domain and represents a storage pool for NHE3 from which it is initially mobilized by α-MD-G. Freeing NHE3 from this pool by reducing NHERF2 allows at least some of this NHE3 to redistribute to the BB. In interpreting the mechanism of these effects, we assume that WGA and biotin fully label the Caco-2 BB [21,22], although if that is not correct, our interpretation would have to be modified to include the intervillus clefts or

lower microvilli as potential storage pools for NHE3. This model is similar to insulin regulation of GLUT4 in identifying a pool of a transporter that is separated from the more general recycling pool and is used for its initial stimulation by insulin [23]. The identification of an intestinal pool of NHE3 that is inactive under basal conditions is similar to the model described for proximal tubule [24], although that location is thought to be in the microvilli above the intervillus clefts and likely involves association with megalin [24–27]. This suggests a similar mechanism of regulation in proximal tubule and intestine, but with differences in location of the storage pool.

Ezrin, which was shown to be needed for α-MD-G stimulation of NHE3 in Caco-2 cells by Turner et al [2–4], also appears to have at least two roles in this stimulation. The α-MD-G–induced increase in p-ezrin occurs similarly in the presence and absence of NHERF2 or its ERM domain (ie, is NHERF2 independent). However, the α-MD-G stimulation of NHE3 activity and amount requires NHERF2 and its ERM domain. We suggest that ezrin along with NHERF2 is involved in holding NHE3 in the apical storage pool from which it is released by α-MD-G. However, ezrin also appears to be taking part in a second aspect of α-MD-G stimulation. After α-MD-G, ezrin continues to be associated with NHE3 at a time that NHERF2 dissociates from NHE3. This is, therefore, likely to involve direct binding of ezrin to NHE3, as we described [14], and probably occurs along the microvilli. It thus is likely to be involved in dispersing NHE3 over the microvilli. We favor this interpretation, since attachment of ezrin to NHERF1 in the microvilli, an alternate role for this ezrin pool, was shown by knockdown in Caco-2 cells (Fig 3) not to be necessary for α-MD-G stimulation of NHE3.

In conclusion, α-MD-G stimulates intestinal NHE3 activity under both basal conditions and in an acute cholera-toxin-induced watery diarrhea model. Both Akt and NHERF2 are required for this regulation. Regulation seems to occur by similar mechanisms in the mouse jejunum and in Caco-2 Na+ absorptive cells. NHERF2 allows α-MD-G stimulation of NHE3 activity through changing NHE3 complexes and regulating NHE3 trafficking, including releasing NHE3 from a storage pool. Two different pools of BB ezrin participate in stimulation of NHE3. These studies have added new insights into how NHE3 is regulated under basal and α-MD-G stimulated conditions which appears relevant for how ORS stimulates intestinal Na absorption and which should be helpful in developing improved therapies for diarrheal diseases.

Supplementary Material

Refer to Web version on PubMed Central for supplementary material.

Acknowledgments

Supported, in whole or in part, NIH Grants R01-DK26523, R01-DK61765, PO1-DK72084, and R24-DK64388

References

1. Zachos NC, Tse M, Donowitz M. Molecular physiology of intestinal Na+/H+ exchanger. Annu Rev Physiol 2005;67:411–443. [PubMed: 15709964]
2. Hu Z, Wang Y, Graham WV, Su L, et al. MAPKAPK-2 is a critical signaling intermediate in NHE3 activation following Na+-glucose cotransport. J Biol Chem 2006;281:24247–24253. [PubMed: 16793766]
3. Turner JR, Black ED. NHE3-dependent cytoplasmic alkalinization is triggered by Na(+)-glucose cotransport in intestinal epithelia. Am J Physiol Cell Physiol 2001;281:C1533–C1541. [PubMed: 11600416]

4. Zhao H, Shiue H, Palkon S, et al. Ezrin regulates NHE3 translocation and activation after Na+-glucose cotransport. Proc Natl Acad Sci U S A 2004;101:9485–9490. [PubMed: 15197272]
5. Shiue H, Musch MW, Wang Y, et al. Akt2 phosphorylates ezrin to trigger NHE3 translocation and activation. J Biol Chem 2005;280:1688–1695. [PubMed: 15531580]
6. Donowitz M, Cha B, Zachos N, et al. NHERF Family and NHE3 regulation. J Physiol 2005;567:3–11. [PubMed: 15905209]
7. Donowitz M, Li X. Regulatory binding partners and complexes of NHE3. Physiol Rev 2007;87:825–872. [PubMed: 17615390]
8. Li X, Zhang H, Cheong A, et al. Carbachol regulation of rabbit ileal brush border Na+-H+ exchanger 3 (NHE3) occurs through changes in NHE3 trafficking and complex formation and is Src dependent. J Physiol 2004;556:791–804. [PubMed: 14978207]
9. Li X, Donowitz M. Fractionation of subcellular membrane vesicles of epithelial and nonepithelial cells by OptiPrep density gradient ultracentrifugation. Methods Mol Biol 2008;440:97–110. [PubMed: 18369940]
10. Broere N, Hillesheim J, Tuo B, et al. Cystic fibrosis transmembrane conductance regulator activation is reduced in the small intestine of Na+/H+ exchanger 3 regulatory factor 1 (NHERF-1)- but not NHERF-2-deficient mice. J Biol Chem 2007;282:37575–37584. [PubMed: 17947234]
11. Murtazina R, Kovbasnjuk O, Zachos NC, et al. Tissue-specific regulation of sodium/proton exchanger isoform 3 activity in Na(+)/H(+) exchanger regulatory factor 1 (NHERF1) null mice. cAMP inhibition is differentially dependent on NHERF1 and exchange protein directly activated by cAMP in ileum versus proximal tubule. J Biol Chem 2007;282:25141–25151. [PubMed: 17580307]
12. Ma T, Thiagarajah JR, Yang H, et al. Verkman Thiazolidinone CFTR inhibitor identified by high-throughput screening blocks cholera toxin–induced intestinal fluid secretion. J Clin Invest 2002;110:1651–1658. [PubMed: 12464670]
13. Sarker R, Grønborg M, Cha B, et al. Casein kinase 2 binds to the C terminus of Na+/H+ exchanger 3 (NHE3) and stimulates NHE3 basal activity by phosphorylating a separate site in NHE3. Mol Biol Cell 2008;19:3859–3870. [PubMed: 18614797]
14. Cha B, Tse M, Yun C, et al. The NHE3 juxtamembrane cytoplasmic domain directly binds ezrin: dual role in NHE3 trafficking and mobility in the brush border. Mol Biol Cell 2006;17:2661–2673. [PubMed: 16540524]
15. Peti-Peterdi J, Toma I, Sipos A, et al. Multiphoton imaging of renal regulatory mechanisms. Physiology (Bethesda) 2009;24:88–96. [PubMed: 19364911]
16. Barnett SF, Defeo-Jones D, Fu S, et al. Identification and characterization of pleckstrin-homology-domain-dependent and isoenzyme-specific akt inhibitors. Biochem J 2005;385:399–408. [PubMed: 15456405]
17. Cha B, Kenworthy A, Murtazina R, et al. The lateral mobility of NHE3 on the apical membrane of renal epithelial OK cells is limited by the PDZ domain proteins NHERF1/2, but is dependent on an intact actin cytoskeleton as determined by FRAP. J Cell Sci 2004;117:3353–3365. [PubMed: 15226406]
18. Madara JL, Pappenheimer JR. Structural basis for physiological regulation of paracellular pathways in intestinal epithelia. J Membr Biol 1987;100:149–164. [PubMed: 3430571]
19. Wade JB, Welling PA, Donowitz M, Shenolikar S, Weinman EJ. Differential renal distribution of NHERF isoforms and their colocalization with NHE3, ezrin, and ROMK. Am J Physiol Cell Physiol 2001;280:C192–C198. [PubMed: 11121391]
20. Cha B, Zhu XC, Chen W, Jones M, Ryoo S, Zachos NC, Chen TE, Lin R, Sarker R, Kenworthy AK, Tse M, Kovbasnjuk O, Donowitz M. NHE3 mobility in brush borders increases upon NHERF2-dependent stimulation by lyophosphatidic acid. J Cell Sci 2010;123:2434–2443. [PubMed: 20571054]
21. Akhter S, Kovbasnjuk O, Li X, et al. Na(+)/H(+) exchanger 3 is in large complexes in the center of the apical surface of proximal tubule-derived OK cells. Am J Physiol Cell Physiol 2002;283:C927–C940. [PubMed: 12176749]

22. Malyukova I, Murray KF, Zhu C, et al. Macropinocytosis in Shiga toxin 1 uptake by human intestinal epithelial cells and transcellular transcytosis. Am J Physiol Gastrointest Liver Physiol 2009;296:G78–G92. [PubMed: 18974311]

23. Xiong W, Jordens I, Gonzalez E, McGraw TE. GLUT4 is sorted to vesicles whose accumulation beneath and insertion into the plasma membfrne are differentially regulated by insulin and selectively affected by insulin resistance. Mol Biol Cell 2010;21:1375–1386. [PubMed: 20181829]

24. Biemesderfer D, DeGray B, Aronson PS. Active (9.6 s) and inactive (21 s) oligomers of NHE3 in microdomains of the renal brush border. J Biol Chem 2001;276:10161–10167. [PubMed: 11120742]

25. McDonough AA, Biemesderfer D. Does membrane trafficking play a role in regulating the sodium/hydrogen exchanger isoform 3 in the proximal tubule? Curr Opin Nephrol Hypertens 2003;12:533–541. [PubMed: 12920402]

26. McDonough AA. Mechanisms of proximal tubule sodium transport regulation that link extracellular fluid volume and blood pressure. Am J Physiol Regul Integr Comp Physiol 2010;298:R851–R861. [PubMed: 20106993]

27. Riquier AD, Lee DH, McDonough AA. Renal NHE3 and NaPi2 partition into distinct membrane domains. Am J Physiol Cell Physiol 2009;296:C900–C910. [PubMed: 19158399]

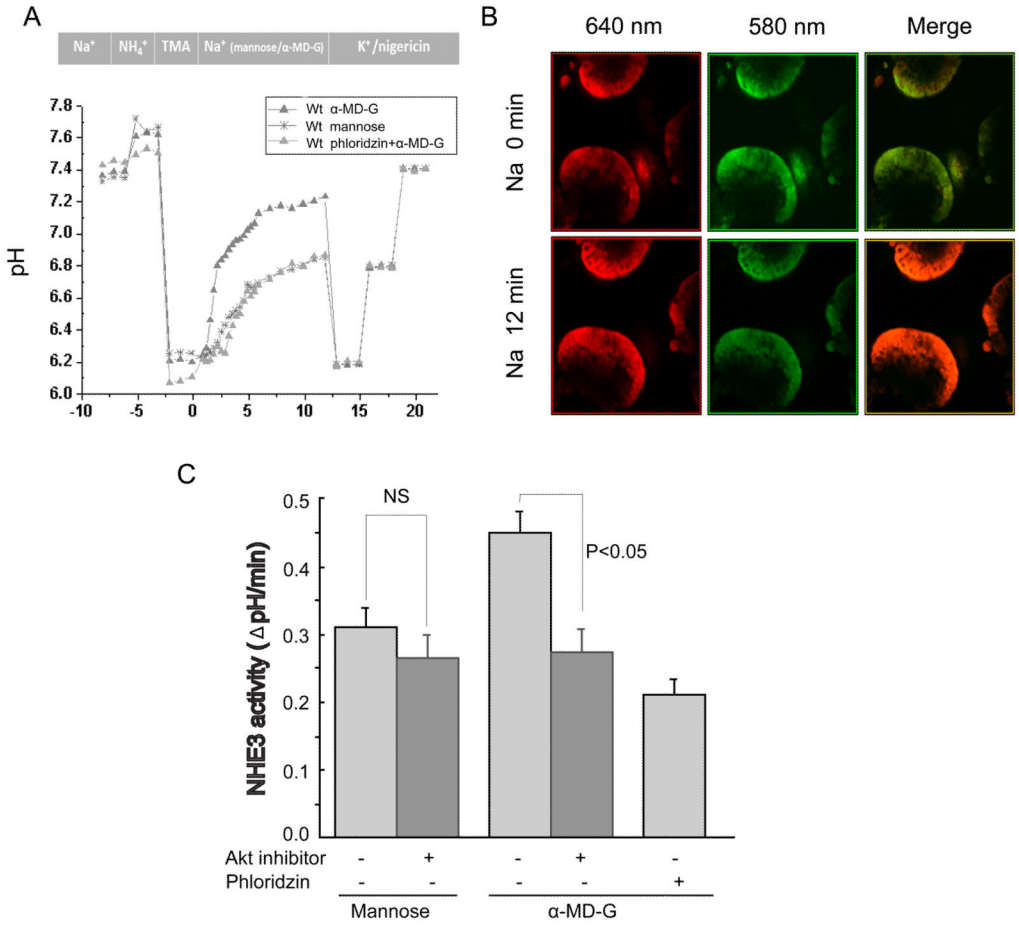

Fig 1. α-Methyl-D-Glucose stimulation of NHE3 requires AKT

A) Murine jejunal pHi determination over time is superimposed on the experimental protocol. After acidification by sequential incubation with NH_4Cl and TMA (MA), the tissue was exposed to Na solution containing 25mM mannose or α-MD-G with fluorescence recorded over 12 min (3 emission ratios obtained per min in the first 5 min and one per min in the following 7 min). The experiment was ended with exposure to 3 pH calibration solutions. B) Images of the two emission (580nm:green; 640nm:red) wavelengths obtained at the beginning and end of Na incubation; the merged image illustrates a change in pHi (presented as color change). C) α-MD-G stimulates NHE3 activity in mouse jejunum via SGLT-1, which is inhibited by exposure to an Akt inhibitor. Results are means ± SEM.

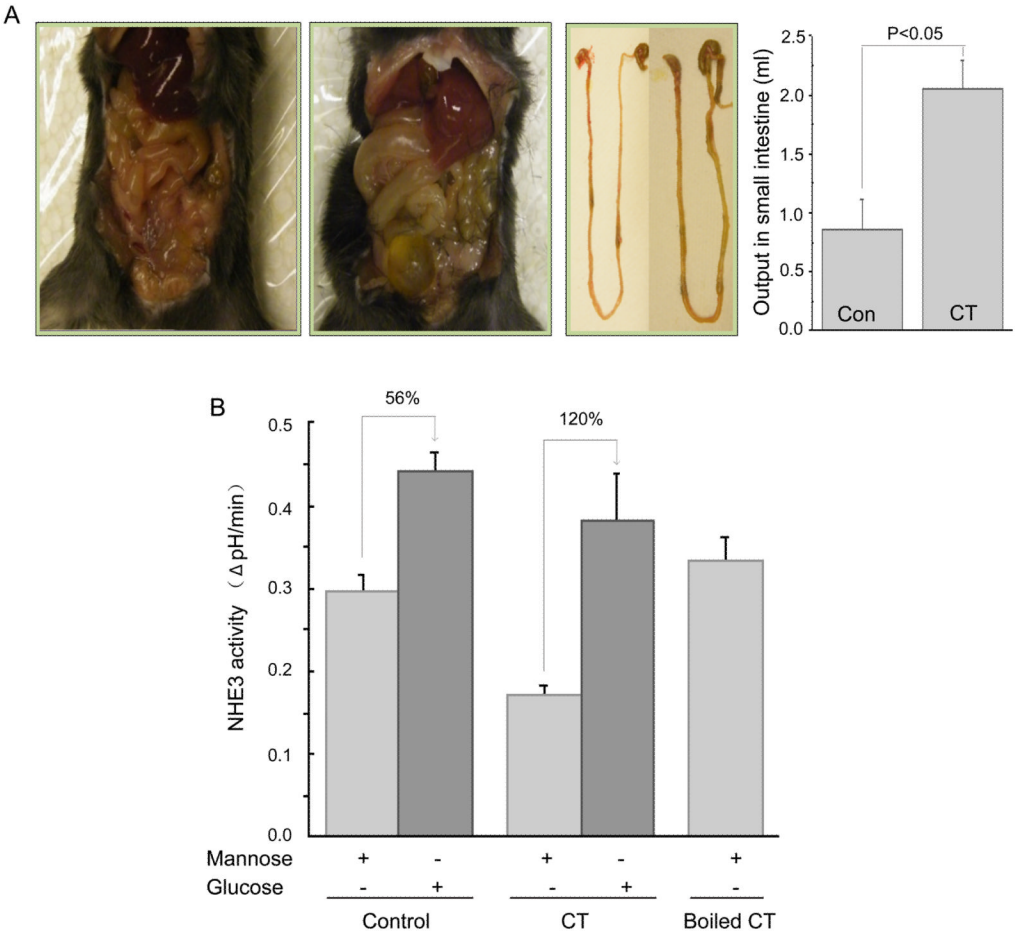

Fig 2. α-MD-G reverses the inhibition of NHE3 activity in an acute CT diarrhea model

A) Increased accumulation of fluid in the small intestine and cecum in a CT-treated animal is shown compared with a control animal. Results are small intestinal fluid, means ± SEM (control, n=3; CT, n=4). P value is comparison of control/CT. B) NHE3 activity was determined by two-photon microscopy/SNARF-4F on the jejunum of these tissues in the presence of D-mannose or α-MD-G. While NHE3 activity was reduced by CT in the presence of mannose, α-MD-G increased NHE3 activity more in the CT jejunum. After α-MD-G exposure, NHE3 activity was similar in the control and CT jejunum.

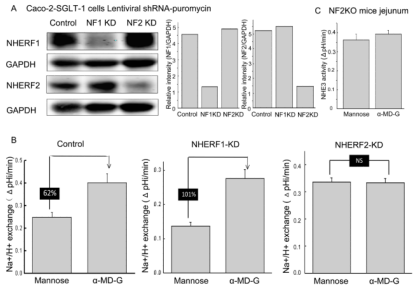

Fig 3. α-MD-G stimulation of NHE3 activity is NHERF2 but not NHERF1 dependent in Caco-2/SGLT1/HA-NHE3 cells

A) NHERF1 and 2 were knocked down by 70–80% without altering the other NHERF. At least five independent KD studies for each NHERF were performed. A single study is shown here. B) α-MD-G caused similar NHE3 stimulation in GFP (control) shRNA and NHERF1 KD Caco-2 cells. In contrast, KD NHERF2 abolished α-MD-G stimulation of NHE3 activity. Results are typical of at least four independent experiments. C) α-MD-G failed to stimulate NHE3 activity compared to D-mannose in NHERF2 KO mouse jejunum, demonstrated by two-photon microscopy. Data shown are means ± SEM (n=5).

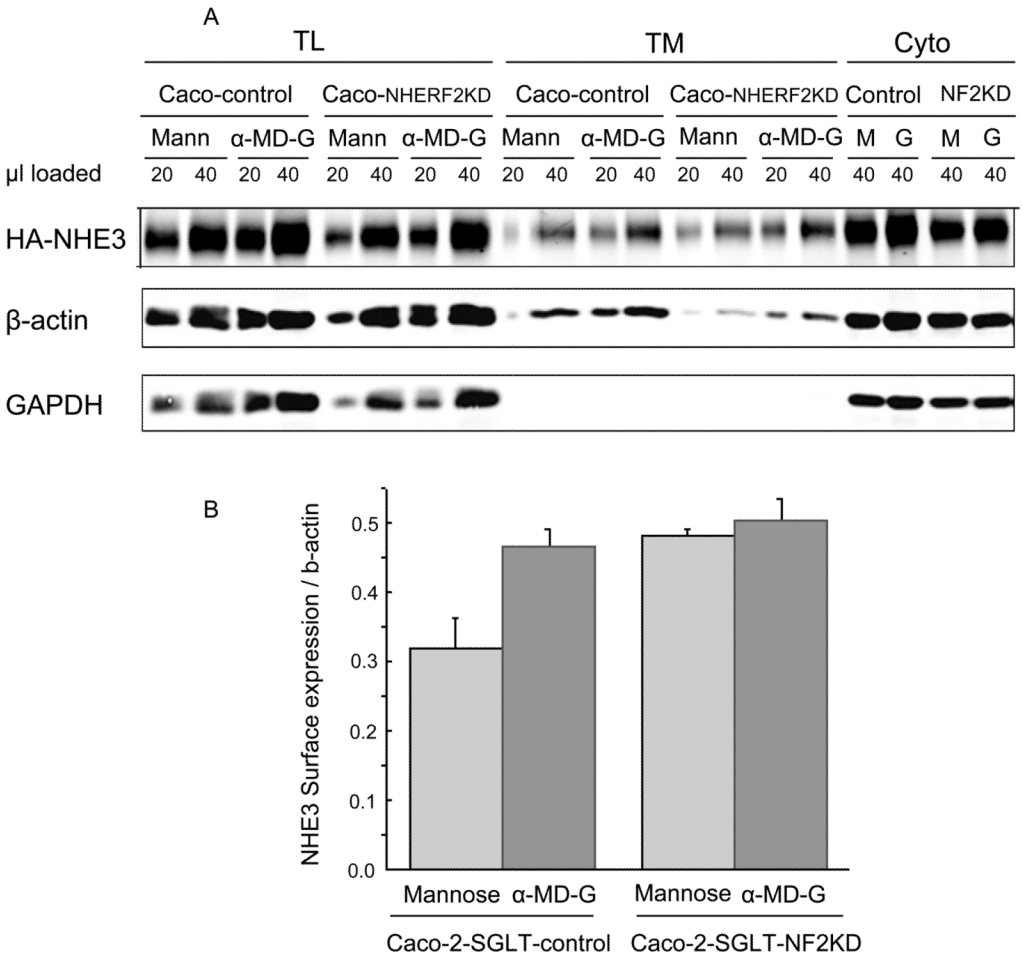

Fig 4. Amount of plasma membrane NHE3 is increased by α-MD-G treatment as determined by surface biotinylation, which is NHERF2 Dependent

A) Caco-2/HA-NHE3/GFP-shRNA and NHERF2 KD cells had amount of BB NHE3 determined. Two dilutions of total cell lysate, avidin precipitate and remaining supernatant were loaded on SDS-PAGE and NHE3, GAPDH and β-actin identified by immunoblotting. B). Results were quantitated using Odyssey (Li-COR). Bar graphs show the calculated means ± SEM of amount of BB NHE3 normalized to β-actin. At least three separate studies were performed for each condition. α-MD-G induced a higher BB expression of NHE3 compared to D-mannose with similar total NHE3 expression. In contrast, in Caco-2/SGLT1/NHERF2 KD cells, there was no significant change in the amount of surface NHE3. There was more surface expression of NHE3 under D-mannose conditions in the NHERF2 KD cells compared to the control group.

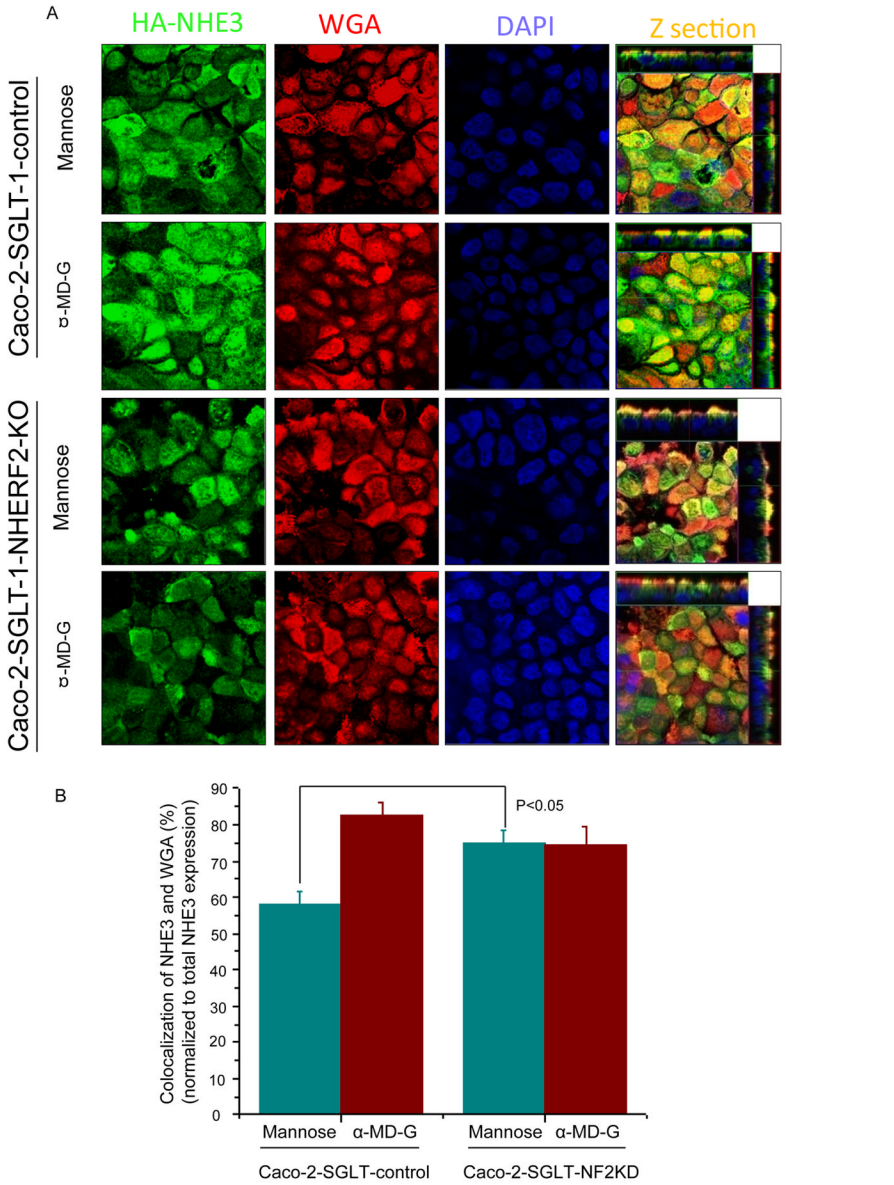

Fig 5. NHERF2 is involved in holding NHE3 localized in a non-WGA accessible pool in basal conditions (mannose treated), which can be mobilized by α-MD-G treatment

A) Caco-2/HA-NHE3/GFP-shRNA and NHERF2KD cells polarized on Anopore filters were treated with mannose or α-MD-G for 5 mins. After fixation with paraformaldehyde at 4°C, cells were exposed to WGA-Texas Red at 4°C. Co-localization of WGA and HA-NHE3 was analyzed by MetaMorph Software. Compared with the mannose group, more NHE3 co-localized with WGA (yellow) after α-MD-G treatment. In Caco-2/NHERF2 KD cells, the co-localization of NHE3 with WGA was similar between mannose and α-MD-G. Mannose-treated Caco-2 cells had less NHE3/WGA co-localization than NHERF2 KD cells ($p<0.05$). B) Bar graphs show the percentage of NHE3 co-localized with WGA normalized to total NHE3 expression. At least four separate images and 20 random, individual areas (Z sections) were analyzed for each group.

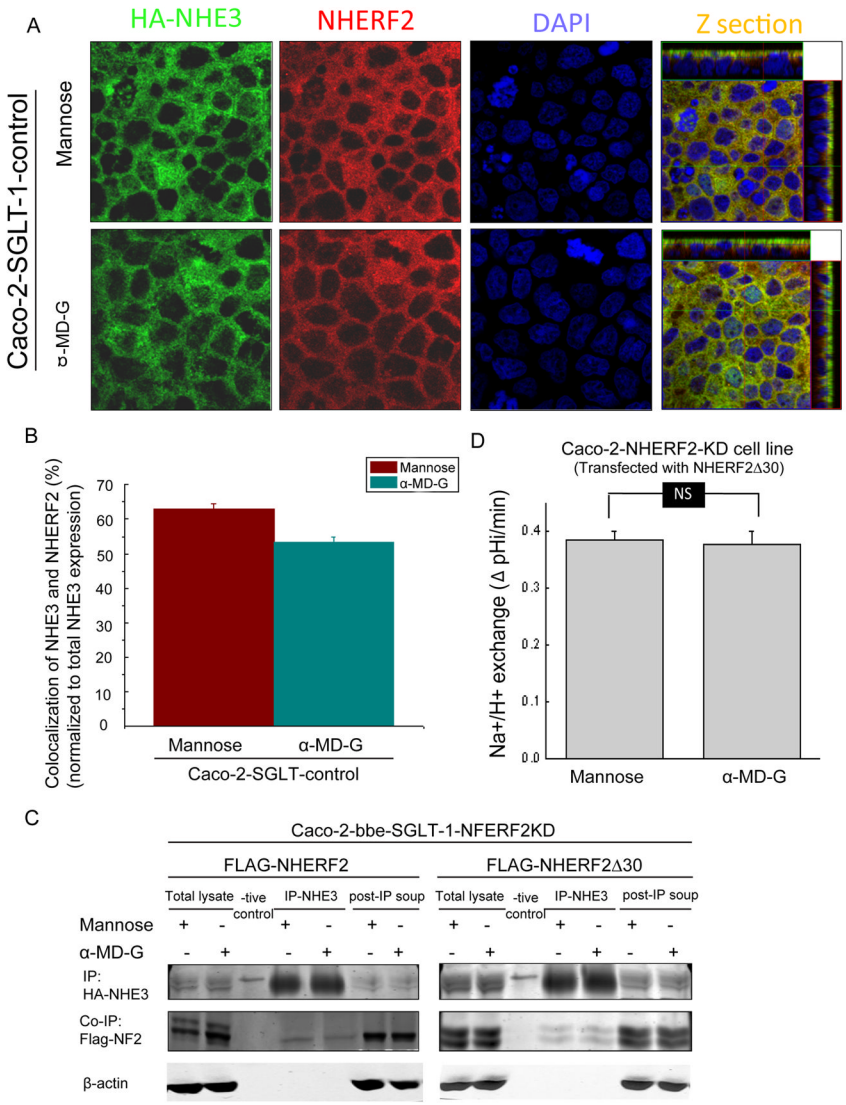

Fig 6. α-MD-G regulation of NHE3 trafficking requires dissociation from NHERF2

A) Caco-2//HA-NHE3 cells were treated with 25 mM D-mannose or α-MD-G and then were fixed and labeled by anti-HA-NHE3 (monoclonal) and anti-NHERF2 (polyclonal antibodies), followed by anti-mouse-FITC and anti-rabbit-Cy3. All images were recorded with the same settings. Co-localization between NHE3/NHERF2 was quantitated by MetaMorph software. A) Typical images of NHE3 (green) and NHERF2 (red) double staining in both D-mannose or α-MD-G treatment. Yellow color shows the co-localization of these two proteins. B) The co-localization of NHE3 and NHERF2 was decreased from 62.8±1.7% to 53.4±1.4% by α-MD-G treatment ($p<0.05$). Bar graphs show the percentage of NHE3 co-localized with NHERF2 compared with total NHE3. C) Dissociation of NHERF2 and NHE3 with short term α-MD-G treatment was demonstrated by co-immunoprecipitation in the Caco-2/NHERF2 but not the NHERF2 Δ30 cell models. α-MD-G treatment reduced the amount of FLAG-NHERF2 co-precipitated when NHE3 was IP. This did not occur when the Caco-2 cells expressed FLAG-NHERFΔ30. Similar results were obtained with 3 duplicate experiments. D) Caco-2/SGLT-1 cells with NHERF2 KD and expressing NHERF2Δ30 were examined for α-MD-G stimulation of NHE3 activity. α-MD-G failed to stimulate NHE3 activity in these cells. N=6.

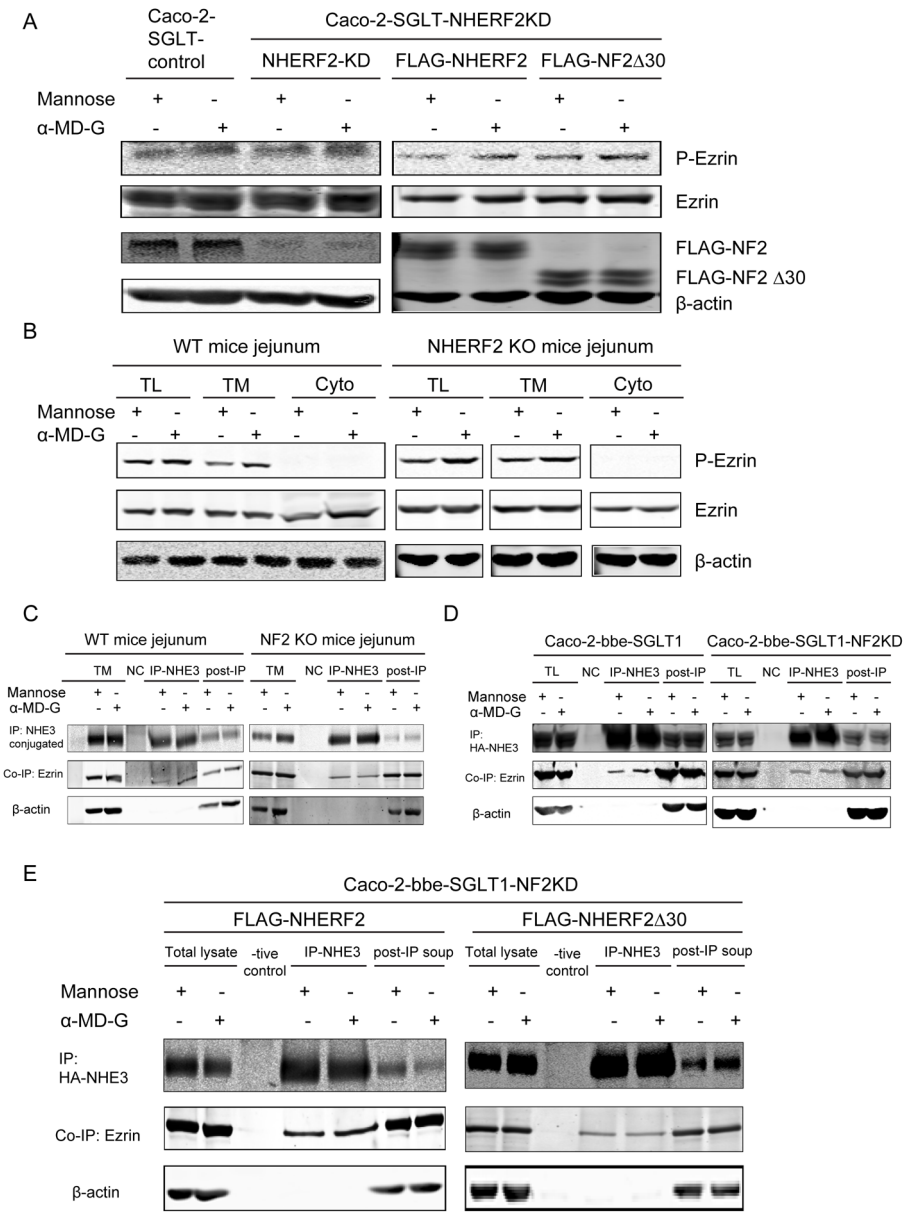

Fig 7.

A,B) α-MD-G-induced ezrin phosphorylation occurs prior to NHERF2 regulation in both Caco-2 cell model and mouse jejunum. The increase of p-ezrin expression with α-MD-G treatment was observed in the Caco-WT, Caco-NF2 KD, Caco-NF2 KD then transfected with NF2, and Caco-NF2 KD then transfected with NF2 Δ30 cell lines, as shown in A. Also in both WT and NF2 KO mice, α-MD-G increased p-ezrin in total membrane and lysate. **C, D) α-MD-G treatment increased the binding between NHE3 and ezrin, which was dependent on NHERF2.** C) The co-immunoprecipitation of ezrin with NHE3 was enhanced with 10 mins α-MD-G treatment in Caco-2 cells with intact NHERF2 but not with NHERF2 KD. D) These results were confirmed with NHE3 co-immunoprecipitation of ezrin increased by α-MD-G in jejunal WT mouse jejunum but not in NHERF2 KO. **E) The ezrin-binding site in NHERF2 is required for α-MD-G -induced stimulation of NHE3-ezrin association.** The increase of NHE3-ezrin co-precipitation occurred in Caco-2 cells

overexpressing NHERF2, but not in those overexpressing NHERF2 Δ30. Similar results were seen in 3 identical experiments.